Available online at www.sciencedirect.com
ScienceDirect
International Journal of Solids and Structures 44 (2007) 1242–1255
INTERNATIONAL JOURNAL OF SOLIDS and STRUCTURES
www.elsevier.com/locate/ijsolstr

Effect of small size on dispersion characteristics of wave in carbon nanotubes

G.Q. Xie [a,b,c], X. Han [a,*], S.Y. Long [b]

[a] *The Key Laboratory of Advanced Technology for Vehicle Body Design and Manufacture of Ministry of Education, Hunan University, Changsha 410082, PR China*
[b] *Department of Engineering Mechanics, Hunan University, Changsha 410082, PR China*
[c] *Civil Engineering & Mechanics college, Xiangtan University, Xiangtan 411105, PR China*

Received 7 April 2006; received in revised form 4 June 2006
Available online 20 June 2006

Abstract

Effect of small size on dispersion characteristics of waves in multi-walled carbon nanotubes is investigated using an elastic shell model. Dynamic governing equations of the carbon nanotube are formulated on the basis of nonlocal elastic theory. The relationship between wavenumber and frequency of wave propagation is obtained from the solution of the eigenvalue equations. The numerical results show that the dispersion characteristics of wave in the multi-walled carbon nanotube are affected by the small size. Effect of small size is not obvious for the smaller wavenumber, and it will arise and increase gradually with the increase of the wavenumber. Effect of the small size will decrease as the inner radius of carbon nanotubes increases. In addition, the explicit expressions of the cut-off frequencies are derived. The results show that the cut-off frequencies cannot be influenced by the small size of carbon nanotubes.

Keywords: Multi-walled carbon nanotube; Elastic wave; Small-size effects; Dispersion

1. Introduction

Carbon nanotubes (CNTs) are regarded as potential nano-structural materials. Engineering applications of CNTs have been reported, such as atomic-force microscope (AFM), field emitters (Fan et al., 1999), nano-fillers for composite materials, micro-electronic devices (Yao et al., 1999; Rueckes et al., 2000), etc. Multi-walled carbon nanotubes can be employed to develop frictionless nano-actuators, nano-motors, nano-bearings, and nano-springs (Lau, 2003).

Due to promising applications, carbon nanotubes have attracted considerable attentions. The main methods used to investigate carbon nanotubes are atomistic simulation, continuum models and multi-scale simulation methods. Atomistic simulation is not good for simulation of physical phenomena occurring on

* Corresponding author. Tel.: +86 731 8823993; fax: +86 731 8821445.
E-mail address: hanxu@hnu.cn (X. Han).

0020-7683/$ - see front matter
doi:10.1016/j.ijsolstr.2006.06.019

a vast range of length scales. The continuum models have become a useful tool for studying CNTs in recent years. So far, continuum mechanics methods have been adopted by Ru (2001), Zhang et al. (2004), Li and Chou (2003a, 2005), Wang et al. (2003) and Qian et al. (2005) to investigate the properties of the carbon nanotube. Multi-scale simulation methods are also used by Shen and Atluri (2004), Kohlhoff et al. (1991) and Gumbsch (1996) to study nano-mechanics.

The dynamics characteristics of carbon nanotubes are increasingly interesting. Li and Chou (2003b, 2004) and Zhang et al. (2005a,b) studied the ultrahigh frequency vibrations of carbon nanotubes. Recently, Wang (2005) and Chakraborty et al. (2006) investigated wave characteristics of CNTs. The studies of Yu et al. (1995); Popov and Doren (2000); Reulet et al. (2000) are focused mainly on single-wall carbon nanotubes. Yoon et al. (2003) studied the wave propagating along double-wall and multi-walled carbon nanotubes. In their works, van der Waals force is modeled via their multiple beam theory. Recently, Mira Mitra and Gopalakrishnan (2006) investigated wave propagation in carbon nanotubes embedded composite using wavelet based spectral finite element. Dong and Wang (2006) studied wave propagation in carbon nanotubes under large deformation. The obtained results show that wave propagation in carbon nanotubes appears in a critical frequency or a cut-off frequency for different wave modes; the effect of shear deformation decreases the value of critical frequency; the critical frequency increases as the matrix stiffness increases; the inertia rotary has an obvious influence on the wave velocity for some wave modes in the higher frequency region.

Nonlocal elasticity has been adopted to study the mechanic properties of carbon nanotubes. Zhang et al. (2005a,b) studied free transverse vibrations of double-walled carbon nanotubes using nonlocal elasticity. Wang and Hu (2005) investigated flexural wave propagation in single-walled carbon nanotubes, their study focuses on the wave dispersion caused not only by the rotary inertia and the shear deformation in the model of a traditional Timoshenko beam, but also by the nonlocal elasticity characterizing the microstructure of carbon nanotubes in a wide frequency range up to THz. Wang (2005) studied wave propagation in carbon nanotubes via nonlocal continuum mechanics. They investigated wave propagation in carbon nanotubes (CNTs) with two nonlocal continuum mechanics models: elastic Euler–Bernoulli and Timoshenko beam models.

In this paper, the elastic shell model of a carbon nanotube is established on the basis of nonlocal elasticity, the dynamic governing equations of the multi-walled carbon nanotubes are formulated. The dispersion curve of the waves propagating in a carbon nanotube is obtained from the solution of the eigenvalue equation. The numerical results show that dispersion properties of wave in multi-walled carbon nanotubes are influenced by the small size. The effect of the small size on dynamic properties of carbon nanotubes will arise and increase with the increase of the wavenumber. The effect of small size will decrease as the inner radius of the carbon nanotube increases.

2. Formulation

2.1. Nonlocal elasticity

In Eringen nonlocal elasticity model (Eringen, 1983a,b), consider that stress at a reference point x in a body is the function of strains of all the points in the near region. This is in accordance with atomic theory of lattice dynamics and experimental observations on phonon dispersion. The most general form of the constitutive equation for nonlocal elasticity involves an integral over the entire region of interest. This integral contains a kernel function that describes the relative influences of strains at various locations on the stress at a given location. It is noted that the classical (local) theory of elasticity can be obtained by neglecting the effects of strains at points other than x.

For homogeneous and isotropic elastic solids, the constitutive equation is

$$\boldsymbol{\sigma}(x) = \mathbf{C}_0 : \int_V \alpha(|\mathbf{x}' - \mathbf{x}|, \tau)\boldsymbol{\varepsilon}(\mathbf{x}')\mathrm{d}V(\mathbf{x}') \tag{1}$$

where symbols ':' is the inner product with double contraction, $\mathbf{C}_0$ is the elastic stiffness matrix of classical isotropic elasticity, $\boldsymbol{\sigma}(\mathbf{x})$ denotes the nonlocal stress tensor at $\mathbf{x}$, and $\boldsymbol{\varepsilon}(\mathbf{x}')$ is the strain tensor at any point $\mathbf{x}'$ in the body. The kernel function $\alpha(|\mathbf{x}' - \mathbf{x}|, \tau)$ is the nonlocal modulus, $|\mathbf{x}' - \mathbf{x}|$ is the Euclidean distance, and $\tau = e_0 a/l$, where e_0 is a constant appropriate to each material, a is an internal characteristic size (e.g. size of C–C bond, lattice spacing, granular distance) and l is an external characteristic size (crack size, wave length etc.). The volume integral in Eq. (1) is over the region V occupied by the body.

The kernel function $\alpha(|\mathbf{x}' - \mathbf{x}|, \tau)$ is given as (Eringen, 1983a,b)

$$\alpha(|\mathbf{x}|, \tau) = (2\pi l^2 \tau^2)^{-1} K_0\left(\sqrt{\mathbf{x} \cdot \mathbf{x}}/l\tau\right) \tag{2}$$

where K_0 is the modified Bessel function.

Combination of Eqs. (1) and (2) can obtain

$$(1 - e_0^2 a^2 \nabla^2)\boldsymbol{\sigma} = \mathbf{C}_0 : \boldsymbol{\varepsilon} \tag{3}$$

2.2. van der Waals pressure

Fig. 1 shows the cylindrical shell model of a multi-walled carbon nanotube of the innermost radius R_1. Material of carbon nanotubes is regarded as homogeneous, isotropic and linear elastic. The coordinate system is chosen in this case: the origin is set on the middle surface of the shell, axial coordinate x, tangent coordinate y, radial coordinate z and displacements in the corresponding coordinate directions u, v, w.

When a wave propagates along a carbon nanotube wall, the nested nanotube does not deflect coaxially. Therefore, the adjacent tubes are coupled with van der Waals interaction. If van der Waals pressure at any point between adjacent tubes is assumed to be a linear function of the jump in deflection at that point. $p_{(i+1)i}$ denotes van der Waals pressure on tube i due to tube $i+1$, which is positive inward, is given by Ru (2001)

$$p_{i(i+1)} = c_i(w_{i+1} - w_i) \tag{4}$$

where w_i is the (inward) deflection of the ith tube, van der Waals interaction coefficient c_i is given as (Ru, 2000)

$$c_i = \frac{320(2R_i)}{0.16d^2} \text{ erg/cm}^2 \tag{5}$$

where $d = 0.142$ nm, $i = 1, 2, \ldots, N-1$, R_i is the inner radii of tube i, 1 erg $= 10^{-7}$ J.

Combination of Eqs. (4) and (5) yields

$$p_{(i+1)i} = -\frac{R_i}{R_{i+1}} p_{i(i+1)} \tag{6}$$

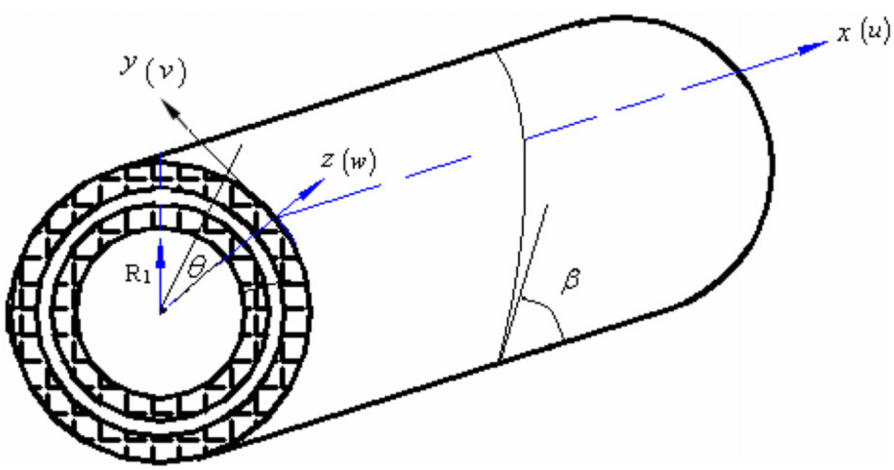

Fig. 1. The shell model of carbon nanotube.

2.3. The basic equations

With the help of Eq. (3), the constitutive equations of the carbon nanotube are

$$\sigma_1 - e_0^2 a^2 \frac{\partial^2 \sigma_1}{\partial x^2} = \frac{E}{1-v^2}[(\varepsilon_1 + \upsilon\varepsilon_2)] \tag{7a}$$

$$\sigma_2 - \frac{e_0^2 a^2}{R^2}\frac{\partial \sigma_2^2}{\partial \theta^2} = \frac{E}{1-v^2}[(\varepsilon_2 + \upsilon\varepsilon_1)] \tag{7b}$$

$$\sigma_{12} - e_0^2 a^2 \left(\frac{\partial^2 \sigma_{12}}{\partial x^2} + \frac{1}{R^2}\frac{\partial^2 \sigma_{12}}{\partial \theta^2}\right) = \frac{E}{2(1+v)}\varepsilon_{12} \tag{7c}$$

where E and υ are Young's modulus and Poisson's ratio of carbon nanotubes, respectively. σ_1 and σ_2 are, respectively, the normal stress in the x-direction and the y-direction. σ_{12} is the shear stress on the xy plane of the middle surface. ε_1, ε_2, ε_{12} represent the in-plane linear strains and shearing strain, respectively. If the small scalar parameter a vanishes, Eq. (7) will revert to Hooke's law of classical elasticity for a planar stress problem.

Geometric equations are

$$\varepsilon_1 = \frac{\partial u}{\partial x}, \quad \varepsilon_2 = \frac{1}{R}\frac{\partial v}{\partial \theta} + \frac{w}{R}, \quad \varepsilon_{12} = \frac{1}{R}\frac{\partial u}{\partial \theta} + \frac{\partial v}{\partial x} \tag{8}$$

The equivalent static stress resultants, obtained from the integration of the stress over the thickness of shell, are given by Hooke's law:

$$N_1 = \sigma_1 h, \quad N_2 = \sigma_2 h, \quad N_{12} = \sigma_{12} h \tag{9a}$$

The equivalent static couples are

$$M_1 = \int_{-h/2}^{h/2} \sigma_1 z\,dz, \quad M_2 = \int_{-h/2}^{h/2} \sigma_2 z\,dz, \quad M_{12} = \int_{-h/2}^{h/2} \sigma_{12} z\,dz \tag{9b}$$

Combination of Eqs. (7a)–(7c), (8), (9a), (9b) yields

$$N_1 = \kappa(\varepsilon_1 + \upsilon\varepsilon_2) + e_0^2 a^2 \frac{\partial^2 N_1}{\partial x^2} = \kappa\left(\frac{\partial u}{\partial x} + \frac{\upsilon}{R}\frac{\partial v}{\partial \theta} + \upsilon\frac{w}{R}\right) + e_0^2 a^2 \kappa\left(\frac{\partial^3 u}{\partial x^3} + \frac{\upsilon}{R}\frac{\partial^3 v}{\partial x^2 \partial \theta} + \frac{\upsilon}{R}\frac{\partial^2 w}{\partial x^2}\right) \tag{10a}$$

$$N_2 = \kappa(\varepsilon_2 + \upsilon\varepsilon_1) + \frac{e_0^2 a^2}{R^2}\frac{\partial^2 N_2}{\partial \theta^2} = \kappa\left(\frac{1}{R}\frac{\partial v}{\partial \theta} + \frac{w}{R} + \upsilon\frac{\partial u}{\partial x}\right) + \frac{e_0^2 a^2}{R^2}\kappa\left(\frac{1}{R}\frac{\partial^3 v}{\partial \theta^3} + \frac{\partial^2 w}{R\partial \theta^2} + \upsilon\frac{\partial^3 u}{\partial \theta^2 \partial x}\right) \tag{10b}$$

$$\begin{aligned} N_{12} &= \frac{\kappa(1-\upsilon)}{2}\varepsilon_{12} + e_0^2 a^2\left(\frac{\partial^2 N_{12}}{\partial x^2} + \frac{\partial^2 N_{12}}{R^2 \partial \theta^2}\right) \\ &= \frac{\kappa(1-\upsilon)}{2}\left(\frac{1}{R}\frac{\partial u}{\partial \theta} + \frac{\partial v}{\partial x}\right) + \frac{\kappa(1-\upsilon)}{2}e_0^2 a^2\left(\frac{1}{R}\frac{\partial^3 u}{\partial x^2 \partial \theta} + \frac{\partial^3 v}{\partial x^3} + \frac{1}{R^3}\frac{\partial^3 u}{\partial \theta^3} + \frac{1}{R^2}\frac{\partial^3 v}{\partial x \partial \theta^2}\right) \end{aligned} \tag{10c}$$

$$\begin{aligned} M_1 &= -D\left(\frac{\partial^2 w}{\partial x^2} + \frac{\upsilon}{R^2}\frac{\partial v}{\partial \theta} + \frac{\upsilon}{R^2}\frac{\partial^2 w}{\partial \theta^2}\right) + e_0^2 a^2 \frac{\partial^2 M_1}{\partial x^2} \\ &= -D\left(\frac{\partial^2 w}{\partial x^2} + \frac{\upsilon}{R^2}\frac{\partial v}{\partial \theta} + \frac{\upsilon}{R^2}\frac{\partial^2 w}{\partial \theta^2}\right) - De_0^2 a^2\left(\frac{\partial^4 w}{\partial x^4} + \frac{\upsilon}{R^2}\frac{\partial^3 v}{\partial x^2 \partial \theta} + \frac{\upsilon}{R^2}\frac{\partial^4 w}{\partial x^2 \partial \theta^2}\right) \end{aligned} \tag{10d}$$

$$\begin{aligned} M_2 &= -D\left(\frac{1}{R^2}\frac{\partial^2 w}{\partial \theta^2} + \frac{1}{R^2}\frac{\partial v}{\partial \theta} + \upsilon\frac{\partial^2 w}{\partial x^2}\right) + \frac{e_0^2 a^2}{R^2}\frac{\partial^2 M_2}{\partial \theta^2} \\ &= -D\left(\frac{1}{R^2}\frac{\partial^2 w}{\partial \theta^2} + \frac{1}{R^2}\frac{\partial v}{\partial \theta} + \upsilon\frac{\partial^2 w}{\partial x^2}\right) - D\frac{e_0^2 a^2}{R^2}\left(\frac{1}{R^2}\frac{\partial^4 w}{\partial \theta^4} + \frac{1}{R^2}\frac{\partial^3 v}{\partial \theta^3} + \upsilon\frac{\partial^4 w}{\partial \theta^2 \partial x^2}\right) \end{aligned} \tag{10e}$$

$$\begin{aligned} M_{12} &= -D(1-\upsilon)\frac{1}{R}\left(\frac{\partial^2 w}{\partial x \partial \theta} + \frac{1}{2}\frac{\partial v}{\partial x}\right) + e_0^2 a^2\left(\frac{\partial^2 M_{12}}{\partial x^2} + \frac{1}{R^2}\frac{\partial M_{12}}{\partial \theta^2}\right) \\ &= -D(1-\upsilon)\frac{1}{R}\left(\frac{\partial^2 w}{\partial x \partial \theta} + \frac{1}{2}\frac{\partial v}{\partial x}\right) - D(1-\upsilon)\frac{e_0^2 a^2}{R}\left(\frac{\partial^4 w}{\partial x^3 \partial \theta} + \frac{1}{2}\frac{\partial^3 v}{\partial x^3} + \frac{1}{R^2}\frac{\partial^4 w}{\partial x \partial \theta^3} + \frac{1}{2R^2}\frac{\partial^3 v}{\partial x \partial \theta^2}\right) \end{aligned} \tag{10f}$$

where

$$\kappa = \frac{Eh}{1-\upsilon^2} \tag{11}$$

$$D = \frac{Eh^3}{12(1-\upsilon^2)} \tag{12}$$

where N_1, N_2 are, respectively, the equivalent static stress resultants in x, y directions. N_{12} is the shearing stress resultant in the middle surface, κ and D are the extensional and the bending rigidity of the shell, respectively.

When the inertial moment is neglected, the equilibrium equations of motion of the multi-walled carbon nanotube are

$$\frac{\partial N_1}{\partial x} + \frac{1}{R}\frac{\partial N_{12}}{\partial \theta} - \rho h \frac{\partial^2 u}{\partial t^2} = 0 \tag{13a}$$

$$\frac{1}{R}\frac{\partial N_2}{\partial \theta} + \frac{\partial N_{12}}{\partial x} + \frac{Q_2}{R} - \rho h \frac{\partial^2 \upsilon}{\partial t^2} = 0 \tag{13b}$$

$$-\frac{N_2}{R} + \frac{\partial Q_1}{\partial x} + \frac{1}{R}\frac{\partial Q_2}{\partial \theta} - \rho h \frac{\partial^2 w}{\partial t^2} - p = 0 \tag{13c}$$

$$\frac{\partial M_{12}}{\partial x} + \frac{1}{R}\frac{\partial M_2}{\partial \theta} - Q_2 = 0 \tag{13d}$$

$$\frac{1}{R}\frac{\partial M_{12}}{\partial \theta} + \frac{\partial M_1}{\partial x} - Q_1 = 0 \tag{13e}$$

where p represents the external forces acting normal to the surface of the shell, in this case, p is van der Walls force. ρ is the mass density of carbon nanotubes. Q_1 and Q_2 are the equivalent static shearing stresses, respectively.

Substitution of Eqs. (8) and (10) into Eq. (13) gets

$$\begin{aligned}
&\frac{\partial^2 u}{\partial x^2} + \frac{\upsilon}{R}\frac{\partial w}{\partial x} + \frac{(1-\upsilon)}{2R^2}\frac{\partial^2 u}{\partial \theta^2} + \frac{(1+\upsilon)}{2R}\frac{\partial^2 \upsilon}{\partial \theta \partial x} + \eta^2\left(\frac{\partial^4 u}{\partial x^4} + \frac{\upsilon}{R}\frac{\partial^3 w}{\partial x^3}\right) + \frac{\eta^2(1+\upsilon)}{2R}\frac{\partial^4 \upsilon}{\partial \theta \partial x^3} \\
&\quad + \frac{(1-\upsilon)\eta^2}{2R^2}\left(\frac{\partial^4 u}{\partial \theta^2 \partial x^2} + \frac{1}{R^2}\frac{\partial^4 u}{\partial \theta^4} + \frac{1}{R}\frac{\partial^4 \upsilon}{\partial \theta^3 \partial x}\right) - \rho\frac{1-\upsilon^2}{E}\frac{\partial^2 u}{\partial t^2} = 0
\end{aligned} \tag{14a}$$

$$\begin{aligned}
&\frac{1}{R^2}\frac{\partial^2 \upsilon}{\partial \theta^2} + \frac{1}{R^2}\frac{\partial w}{\partial \theta} + \frac{\eta^2}{R^3}\left(\frac{1}{R}\frac{\partial^4 \upsilon}{\partial \theta^4} + \frac{1}{R}\frac{\partial^3 w}{\partial \theta^3} + \upsilon\frac{\partial^4 u}{\partial \theta^3 \partial x}\right) + \frac{\eta^2(1-\upsilon)}{2}\chi + \frac{(1-\upsilon)}{2}\left(\frac{1}{R}\frac{\partial^2 u}{\partial \theta \partial x} + \frac{\partial^2 \upsilon}{\partial x^2}\right) \\
&\quad - \frac{h^2}{12R^2}\left(\frac{\partial^3 w}{R^2 \partial \theta^3} + \frac{1}{R^2}\frac{\partial^2 \upsilon}{\partial \theta^2} + \upsilon\frac{\partial^3 w}{\partial x^2 \partial \theta}\right) - \frac{h^2\eta^2}{12R^4}\left(\frac{\partial^5 w}{R^2 \partial \theta^5} + \frac{1}{R^2}\frac{\partial^4 \upsilon}{\partial \theta^4} + \upsilon\frac{\partial^5 w}{\partial x^2 \partial \theta^3}\right) \\
&\quad - \frac{h^2(1-\upsilon)}{12R^2}\left(\frac{\partial^3 w}{\partial \theta \partial x^2} + \frac{1}{2}\frac{\partial^2 \upsilon}{\partial x^2}\right) + \frac{\upsilon}{R}\frac{\partial^2 u}{\partial \theta \partial x} - \frac{h^2(1-\upsilon)\eta^2}{12R^2}\varpi - \frac{\rho(1-\upsilon^2)}{E}\frac{\partial^2 \upsilon}{\partial t^2} = 0
\end{aligned} \tag{14b}$$

$$\begin{aligned}
&-\frac{1}{R^2}\frac{\partial \upsilon}{\partial \theta} - \frac{h^2(1-\upsilon)}{6R^2}\left(\frac{\partial^4 w}{\partial x^2 \partial \theta^2} + \frac{1}{2}\frac{\partial^3 \upsilon}{\partial x^2 \partial \theta}\right) - \frac{(1-\upsilon)h^2\eta^2}{6R^2}\zeta - \frac{\upsilon}{R}\frac{\partial u}{\partial x} - \frac{h^2\eta^2}{12R^2}\vartheta - \frac{w}{R^2} \\
&\quad - \frac{h^2\eta^2}{12}\xi - \frac{h^2}{12R^2}\left(\frac{\partial^4 w}{R^2 \partial \theta^4} + \frac{1}{R^2}\frac{\partial^3 \upsilon}{\partial \theta^3} + \upsilon\frac{\partial^4 w}{\partial \theta^2 \partial x^2}\right) - \frac{\eta^2}{R^3}\left(\frac{1}{R}\frac{\partial^3 \upsilon}{\partial \theta^3} + \frac{1}{R}\frac{\partial^2 w}{\partial \theta^2} + \upsilon\frac{\partial^3 u}{\partial \theta^2 \partial x}\right) \\
&\quad - \frac{h^2}{12}\left(\frac{\partial^4 w}{\partial x^4} + \frac{\upsilon}{R^2}\frac{\partial^3 \upsilon}{\partial \theta \partial x^2} + \frac{\upsilon}{R^2}\frac{\partial^4 w}{\partial x^2 \partial \theta^2}\right) - \frac{(1-\upsilon^2)p}{Eh} - \frac{\rho(1-\upsilon^2)}{E}\frac{\partial^2 w}{\partial t^2} = 0
\end{aligned} \tag{14c}$$

where

$$\eta = e_0 a$$

$$\chi = \frac{\partial^4 u}{R \partial \theta \partial x^3} + \frac{\partial^4 \upsilon}{\partial x^4} + \frac{1}{R^3}\frac{\partial^4 u}{\partial \theta^3 \partial x} + \frac{1}{R^2}\frac{\partial^4 \upsilon}{\partial \theta^2 \partial x^2}$$

$$\varpi = \frac{\partial^5 w}{\partial\theta\,\partial x^4} + \frac{1}{2}\frac{\partial^4 v}{\partial x^4} + \frac{1}{R^2}\frac{\partial^5 w}{\partial\theta^3\,\partial x^2} + \frac{1}{2R^2}\frac{\partial^4 v}{\partial\theta^2\,\partial x^2}$$

$$\xi = \frac{\partial^6 w}{\partial x^6} + \frac{\upsilon}{R^2}\frac{\partial^5 v}{\partial\theta\,\partial x^4} + \frac{\upsilon}{R^2}\frac{\partial^6 w}{\partial x^4\,\partial\theta^2}$$

$$\zeta = \frac{\partial^6 w}{\partial x^4\,\partial\theta^2} + \frac{1}{2}\frac{\partial^5 v}{\partial x^4\,\partial\theta} + \frac{1}{R^2}\frac{\partial^6 w}{\partial x^2\,\partial\theta^4} + \frac{1}{2R^2}\frac{\partial^5 v}{\partial x^2\,\partial\theta^3}$$

$$\vartheta = \frac{1}{R^4}\frac{\partial^6 w}{\partial\theta^6} + \frac{1}{R^4}\frac{\partial^5 v}{\partial\theta^5} + \frac{\upsilon}{R^2}\frac{\partial^6 w}{\partial\theta^4\,\partial x^2}$$

If the small scalar parameter a vanishes, Eq. (14) will revert to the dynamics equations of classical elasticity for a planar stress problem.

2.4. Dispersion equations

Supposing a helical harmonic wave propagates in a multi-walled carbon nanotube, the displacement field as complex exponential form of a harmonic place wave

$$\mathbf{u}(x,\theta,t) = \mathbf{U}\exp(\mathrm{j}n\theta + \mathrm{j}k_x x - \mathrm{j}\omega t) \tag{15}$$

where $\mathbf{u} = (u, v, w)^{\mathrm{T}}$, $\mathbf{U} = (U, V, W)^{\mathrm{T}}$ are the amplitude of displacement in the three coordination directions, $\mathrm{j}^2 = -1$, ω is the angular frequency of wave, n is the component of wavenumber in the direction y, k_x is the component of wavenumber in the direction x.

$$n = Rk\sin\beta \tag{16}$$

$$k_x = k\cos\beta \tag{17}$$

where β is the angle of the propagation direction of the wave with respect to axial direction.

Substitution of Eq. (15) into Eq. (14) obtains the governing equation of the ith wall

$$[\mathbf{K}_i - \omega^2\mathbf{M}_i]\mathbf{U}_i = \mathbf{q}_i \tag{18}$$

where $\mathbf{M}_i$, $\mathbf{K}_i$ and $\mathbf{q}_i$ are given in Appendix A, $\mathbf{q}_i$ is the coupled terms due to van der Waals interaction.

Assembling of Eq. (18), the total equation of the N-wall carbon nanotube can be obtained

$$[\mathbf{K}_t - \omega^2\mathbf{M}_t]\mathbf{U}_t = \mathbf{0} \tag{19}$$

where $\mathbf{K}_t$ is $3N \times 3N$ total stiffness matrix, $\mathbf{M}_t$ is $3N \times 3N$ total mass matrix, $\mathbf{U}_t$ is $3N$ total displace amplitude vector, $\mathbf{q}_i$ of Eq. (18) is incorporated into $\mathbf{K}_t$, they are given in Appendix B. The relationship between the wavenumbers k and frequencies ω is obtained from the condition for the nonzero solution of U_t in Eq. (19) as follows:

$$|\mathbf{K}_t - \omega^2\mathbf{M}_t| = \mathbf{0} \tag{20}$$

According to a given wavenumber k, the corresponding frequency ω can be determined from Eq. (20). Thus, for different helical angle, dispersion curves of wave propagation in MWNTs are obtained.

For the mth mode, the Rayleigh quotient can be written as

$$\omega_m^2 = \frac{\varphi_m^{\mathrm{L}}\mathbf{K}_t\varphi_m^{\mathrm{R}}}{\varphi_m^{\mathrm{L}}\mathbf{M}_t\varphi_m^{\mathrm{R}}} \tag{21}$$

where φ_m^{L} and φ_m^{R} are the mth transposed left and right eigenvectors of Eq. (19).

Phase velocity represents the rate at which energy is transported, and it is given as (Achenbach, 1973)

$$c_g = \frac{\omega}{k} \tag{22}$$

2.5. Cut-off frequency

Substituting $k = 0$ into Eq. (20), the two cut-off frequencies of the two-walled carbon nanotube can be obtained

$$\omega_{\mathrm{cut1}} = \sqrt{\frac{E\left[2\frac{(1-\upsilon^2)c_1}{Eh} + \frac{\left(R_1^2+R_2^2\right)}{R_1^2R_2^2}\right] - \sqrt{4\left[\frac{(1-\upsilon^2)c_1}{Eh}\right]^2 + \frac{\left(R_1^2+R_2^2\right)^2}{R_1^4R_2^4} - \frac{4}{R_1^2R_2^2}}}{2\rho(1-\upsilon^2)}} \tag{23a}$$

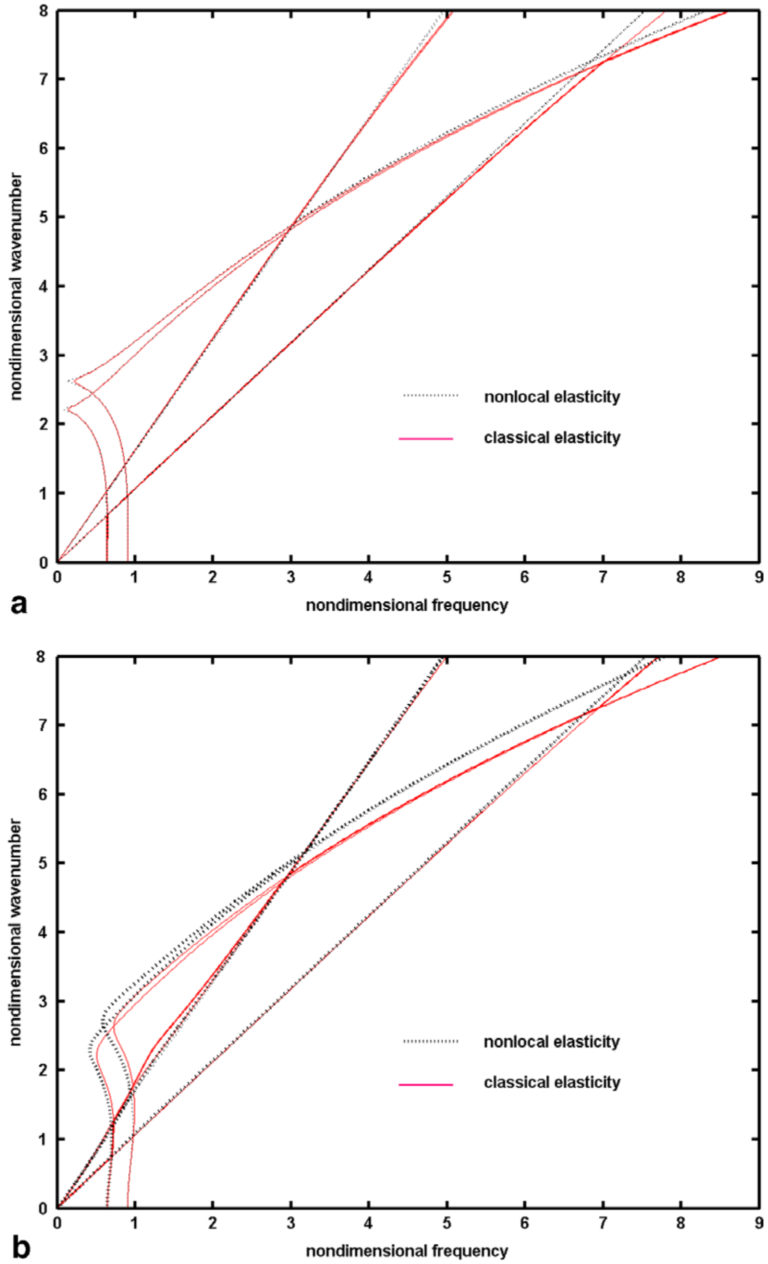

Fig. 2. The dispersion curve of the two-wall carbon nanotube. (a) $\beta = 0°$, $R = 0.8$ nm; (b) $\beta = 30°$, $R = 0.8$ nm.

$$\omega_{\mathrm{cut}2} = \sqrt{\frac{E\left[2\frac{(1-\upsilon^2)c_1}{Eh} + \frac{\left(R_1^2+R_2^2\right)}{R_1^2R_2^2}\right] + \sqrt{4\left[\frac{(1-\upsilon^2)c_1}{Eh}\right]^2 + \frac{\left(R_1^2+R_2^2\right)^2}{R_1^4R_2^4} - \frac{4}{R_1^2R_2^2}}}{2\rho(1-\upsilon^2)}} \tag{23b}$$

Cut-off frequencies of the three-walled carbon nanotube can be obtained in the same way.

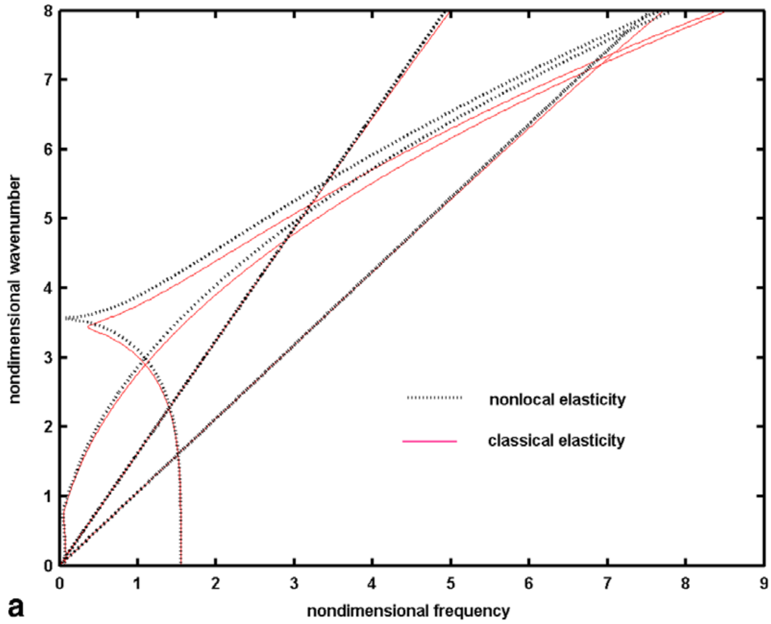

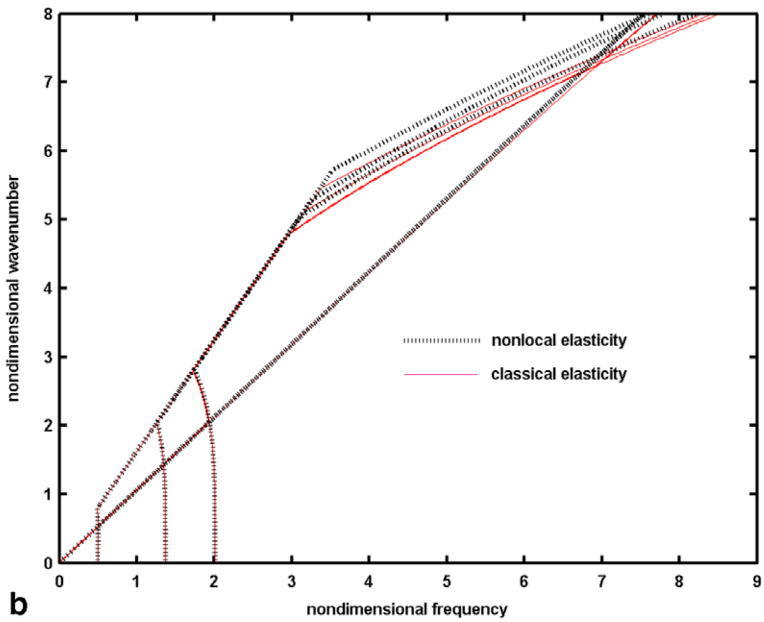

Fig. 3. The dispersion curve of the carbon nanotube $\beta = 30°$, $R = 10$ nm. (a) The two-walled carbon nanotube, (b) the three-walled carbon nanotube.

3. Numerical examples

For all the subsequent numerical examples, carbon nanotubes are taken with the in-plane stiffness $Eh = 360\ \mathrm{J/m^2}$ given by Yakobson et al. (1996), thickness of the carbon nanotube $h = 0.34$ nm, length of C–C bond $a = 0.142$ nm and mass density $\rho = 2.3 \times 10^3\ \mathrm{kg/m^3}$ (Yoon et al., 2004), $e_0 = 0.39$ (Eringen, 1983a,b), Poisson's ratio $\upsilon = 0.145$, Young's modulus $E = 1$ TPa.

To investigate the effect of the small size on the dispersion characteristic of the carbon nanotube, we present two numerical examples. One is a two-wall carbon nanotube, another is a three-wall carbon nanotube.

3.1. Case I: two-walled carbon nanotube

Fig. 2(a) and (b) shows that the dispersion curves of the waves propagation in the axial and helical directions along the two-walled carbon nanotube of the inner radius, respectively. It can be seen from these figures that there are two cut-off frequencies of waves. The two cut-off frequencies of the two-walled carbon nanotube of the inner radius 0.8 nm are determined from Eqs. (23a) and (23b), they are 1.8486×10^{13} Hz and 2.6343×10^{13} Hz. It can be found from Eqs. (23a) and (23b) and Fig. 2(a) and (b) that the cut-off frequencies of the carbon nanotube cannot be influenced by the small size of the carbon nanotube. It is also observed from the two figures that the effect of the small size on the dispersion properties of the two-walled carbon nanotube does not arise when the wavenumbers are lower. The effect of the small size will arise and increase gradually with increase of the wavenumbers. This can be explained as follows: the nonlocal theory incorporates big range interactions between particles in a continuum model. Such big range interactions occur between charged atoms or molecules in a solid. Big range forces may also be considered to propagate along fibers or lamina in a composite material (Ilcewicz et al., 1981). Effect of the small size is caused by big range interaction among atoms. The interaction, namely, effect of the small size, will disappear when the distance between two atoms exceeds a critical size. The lower wavenumber corresponds to the longer wavelength; effect of the small size will disappear when the size of the double-walled carbon nanotube covered by the longer wavelength exceeds the critical size. Eringen and Kim (1977) found that nonlocal theory reduces to classical in long wavelength limit and to atomic lattice dynamics in the short wavelength limit. The result of this paper is also in excellent agreement with their results.

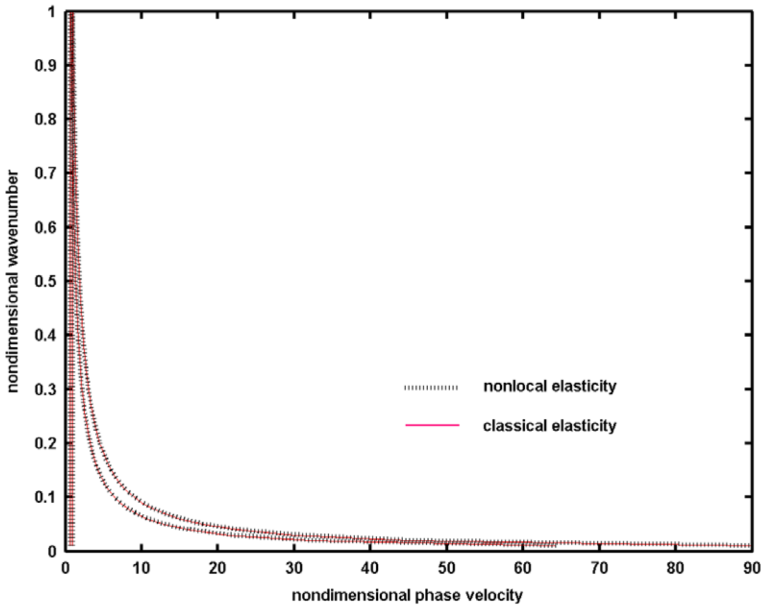

Fig. 4. The phase velocity of the two-wall carbon nanotube $\beta = 30°$, $R = 0.8$ nm.

Fig. 3(a) shows that the dispersion curves of the waves in a two-walled carbon nanotube of the inner radius 10 nm. It is obvious from the comparison between Figs. 2(b) and 3(a) that the effect of the small size on the dispersion characteristics of the two-walled carbon nanotubes will decrease as the inner radius of the carbon nanotube increases.

Fig. 4 shows that phase velocities of the two-walled carbon nanotube of the inner radius 0.8 nm. It is observed from Fig. 4 that at the two cut-off frequencies the wavenumber becomes zero and the corresponding phase velocity of the two-walled carbon nanotube becomes infinite. For the first and second wave modes, the wave velocities remain at an identical constant value for any wavenumber. When the wavenumber is upper,

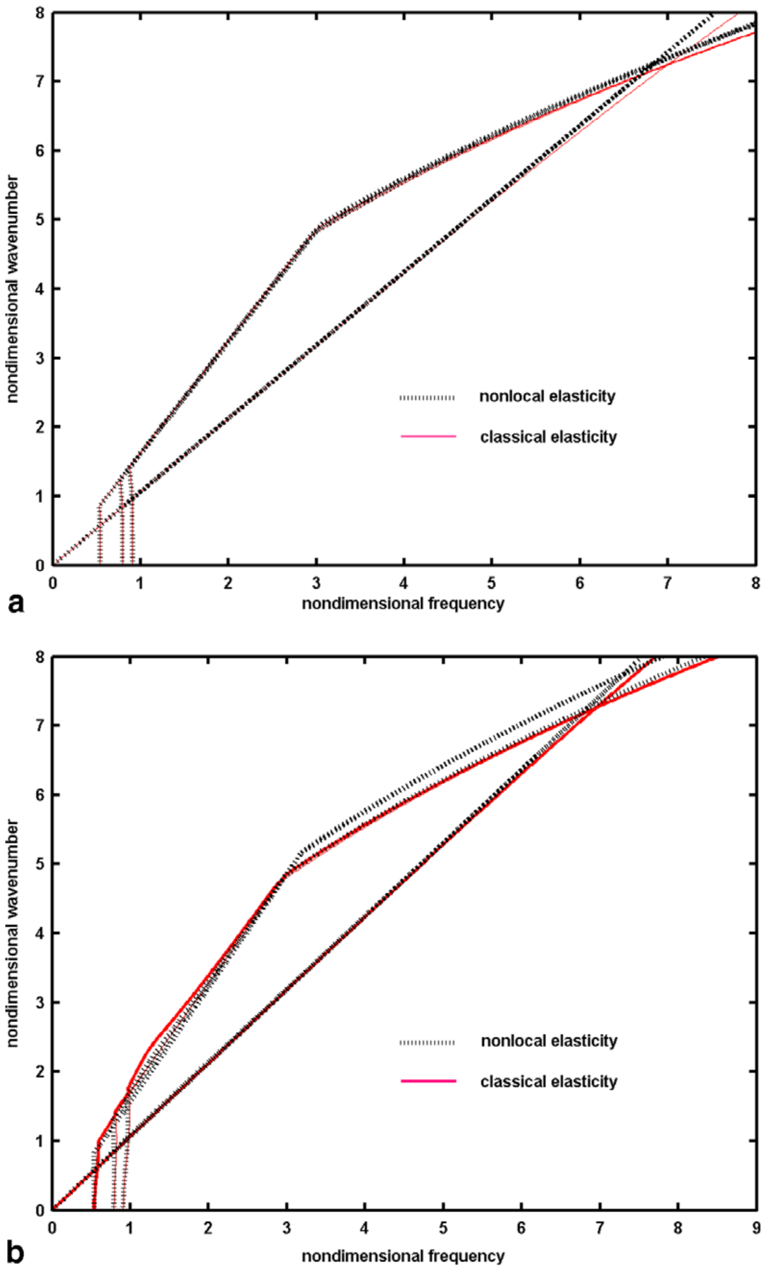

Fig. 5. The dispersion curve of the three-wall carbon nanotube. (a) $\beta = 0°$, $R = 0.8$ nm; (b) $\beta = 30°$, $R = 0.8$ nm.

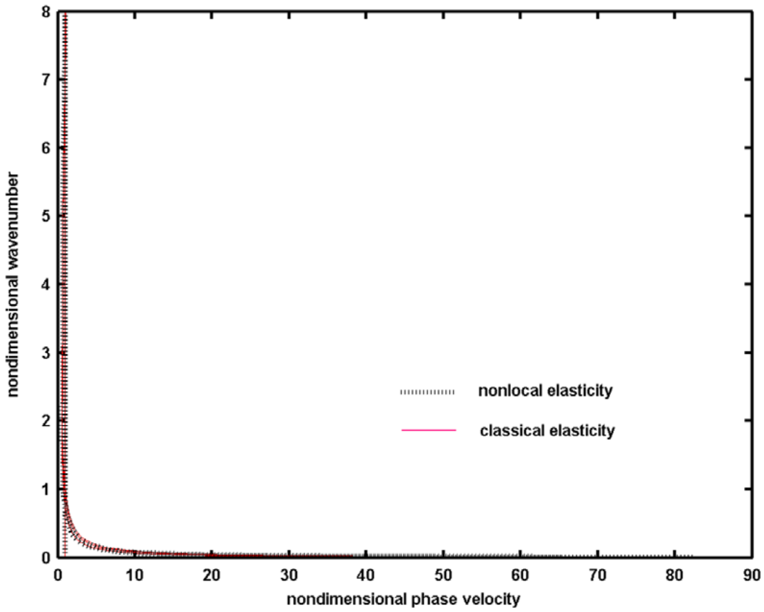

Fig. 6. The phase velocity of the three-wall carbon nanotube $\beta = 30°$, $R = 0.8$ nm.

the wave propagation for the fifth and sixth wave modes appear at a fairly constant velocity, but a sharp drop is observed at k close to zero.

3.2. Case II: three-walled carbon nanotube

Fig. 5(a) shows that the dispersive curves of the three-walled carbon nanotube of the inner radius 0.8 nm. It can be found from the two figures that there are three cut-off frequencies of waves in the three-walled carbon nanotube. It is also observed from these figures that the effect of the small size on the dispersion properties of the three-walled carbon nanotube does not arise when the wavenumbers are lower, and the effect of the small size will emerge and increase gradually with increase of the wavenumbers.

Fig. 5(b) shows that the dispersion curves of the double-walled carbon nanotube of the inner radius 10 nm. It can be seen from the comparison between Figs. 5(b) and 3(b) that the effect of the small size on the dispersion characteristics of the three-walled carbon nanotubes will decrease as the inner radius increases.

Fig. 6 shows that phase velocities of the three-walled carbon nanotube of the inner radius 0.8 nm. It is observed from Fig. 6 that at the three cut-off frequencies the wavenumber becomes zero and the corresponding phase velocity of the three-walled carbon nanotube becomes infinite. For the first three wave modes, the wave velocities remain at the same constant value for any wavenumber. When the wavenumber is bigger, the wave propagation for the fifth, sixth and seventh wave modes appear in a fairly constant velocity, but a sharp drop is found near at $k = 0$.

4. Conclusions

Dynamic equations of the carbon nanotube are obtained on the basis of nonlocal elastic theory. Dispersion characteristics and phase velocity of wave in the carbon nanotube are obtained from the solution of the eigenvalue equations. The numerical results show that the wave characteristics of a carbon nanotube are influenced by the effect of the small scalar size. It has been found that the effect of the small scalar size on the wave properties of the carbon nanotube will increase with the increase of the wavenumber. The effect of the small size on the properties of wave in the carbon nanotube will decrease as the innermost radius of the carbon nanotube increases. The cut-off frequencies cannot be influenced by the small size of the carbon nanotube.

Acknowledgement

This work is supported by the National 973 No. 2004CB719402, NCET-04-0766 and the National Science Foundation of China under the Grant Number 10372031 and 10572048.

Appendix A

$$\mathbf{K}_i = \begin{bmatrix} k_{11}^{(i)} & k_{12}^{(i)} & k_{13}^{(i)} \\ k_{21}^{(i)} & k_{22}^{(i)} & k_{23}^{(i)} \\ k_{31}^{(i)} & k_{32}^{(i)} & k_{33}^{(i)} \end{bmatrix}$$

$$k_{11}^{(i)} = k^2\cos^2\beta + \frac{1-\upsilon}{2}k^2\sin^2\beta - \frac{1-\upsilon}{2}\eta^2k^4\sin^2\beta - \eta^2k^4\cos^4\beta$$

$$k_{12}^{(i)} = \frac{1+\upsilon}{2}k^2\sin\beta\cos\beta - \frac{\eta^2(1+\upsilon)}{2}k^4\cos^3\beta\sin\beta - \frac{\eta^2(1-\upsilon)}{2}k^4\cos\beta\sin^3\beta$$

$$k_{13}^{(i)} = \left(-\frac{\eta^2\upsilon}{R}k^3\cos^3\beta + \frac{\upsilon}{R}k\cos\beta\right)j$$

$$k_{21}^{(i)} = \frac{1+\upsilon}{2}k^2\sin\beta\cos\beta - \frac{\eta^2(1+\upsilon)}{2}k^4\cos^3\beta\sin\beta - \frac{\eta^2(1-\upsilon)}{2}k^4\cos\beta\sin^3\beta$$

$$k_{22}^{(i)} = k^2\sin^2\beta\left(1-\frac{h^2}{12R^2}\right) + \frac{1-\upsilon}{2}k^2\cos^2\beta - \eta^2k^4\sin^4\beta\left(1-\frac{h^2}{12R^2}\right)$$
$$-\frac{\eta^2(1-\upsilon)}{2}k^4\cos^2\beta + \frac{h^2\eta^2(1-\upsilon)}{24R^2}k^4\cos^2\beta - \frac{h^2(1-\upsilon)}{24R^2}k^2\cos^2\beta$$

$$k_{23}^{(i)} = \left(-\frac{1}{R}k\sin\beta - \frac{h^2k^3}{12R}\sin\beta + \frac{\eta^2}{R}k^3\sin^3\beta + \frac{h^2\eta^2}{12R}k^5\sin^3\beta + \frac{\eta^2h^2k^5}{12R}(1-\upsilon)\sin^5\beta\cos\beta\right)j$$

$$k_{31}^{(i)} = \left(\frac{\upsilon}{R}k\cos\beta - \frac{\eta^2}{R}\upsilon k^3\sin^2\beta\cos\beta\right)j$$

$$k_{32}^{(i)} = \left(+\frac{1}{R}k\sin\beta - \frac{h^2k^3}{12R}\sin\beta - \frac{\eta^2}{R}k^3\sin^3\beta + \frac{h^2\eta^2}{12R}k^5\sin^5\beta\right.$$
$$\left.+\frac{h^2\eta^2(1-\upsilon)}{12R}k^5\cos^2\beta\sin\beta + \frac{h^2\eta^2\upsilon}{12R}k^5\cos^2\beta\sin^3\beta\right)j$$

$$k_{33}^{(i)} = +\frac{h^2}{6}k^4\cos^2\beta\sin^2\beta + \frac{h^2}{12}k^4(\cos^4\beta+\sin^4\beta) + \frac{1}{R^2} - \frac{\eta^2h^2}{6}k^6\sin^2\beta\cos^2\beta$$
$$-\frac{h^2\eta^2}{12}k^6(\cos^6\beta+\sin^6\beta - v\cos^2\beta\sin^2\beta) - \frac{\eta^2}{R^2}k^2\sin^2\beta$$

$$\mathbf{M}_i = \mathrm{diag}\left[\frac{\rho(1-\upsilon^2)}{E}\right]_{3\times3}$$

$$\mathbf{q}_i = \left[0, 0, \frac{1-\upsilon^2}{Eh}c_i(W_{i+1}-W_i)\right]^{\mathrm{T}} = [0, 0, C_i(W_{i+1}-W_i)]^{\mathrm{T}}$$

Appendix B

$$\mathbf{M}_t = \mathbf{I}\frac{\rho(1-\upsilon^2)}{E}$$

where $\mathbf{I}$ is $3N\times3N$ identity matrix.

$$\mathbf{U}_t = \begin{bmatrix} u^{(1)} & v^{(1)} & w^{(1)} & u^{(2)} & v^{(2)} & w^{(2)} & \cdots & u^{(N)} & v^{(N)} & w^{(N)} \end{bmatrix}^{\mathrm{T}}$$

$$\mathbf{K}_t = \begin{bmatrix} k_{11}^{(1)} & k_{12}^{(1)} & k_{13}^{(1)} & 0 & 0 & 0 & 0 & 0 & 0 & \cdots \\ k_{21}^{(1)} & k_{22}^{(1)} & k_{23}^{(1)} & 0 & 0 & 0 & 0 & 0 & 0 & \cdots \\ k_{31}^{(1)} & k_{32}^{(1)} & \left(k_{33}^{(1)} + C_1\right) & 0 & 0 & -C_1 & 0 & 0 & 0 & \cdots \\ 0 & 0 & 0 & k_{11}^{(2)} & k_{12}^{(2)} & k_{13}^{(2)} & 0 & 0 & 0 & \cdots \\ 0 & 0 & 0 & k_{21}^{(2)} & k_{22}^{(2)} & k_{23}^{(2)} & 0 & 0 & 0 & \cdots \\ 0 & 0 & -C_1 & k_{31}^{(2)} & k_{32}^{(2)} & \left(k_{33}^{(2)} + C_1 + C_2\right) & 0 & 0 & -C_2 & \cdots \\ 0 & 0 & 0 & 0 & 0 & 0 & k_{11}^{(3)} & k_{12}^{(3)} & k_{13}^{(3)} & \cdots \\ 0 & 0 & 0 & 0 & 0 & 0 & k_{21}^{(3)} & k_{22}^{(3)} & k_{23}^{(3)} & \cdots \\ 0 & 0 & 0 & 0 & 0 & -C_2 & k_{31}^{(3)} & k_{32}^{(3)} & \left(k_{33}^{(3)} + C_1 + C_2 + \cdots\right) & \cdots \\ \vdots & \vdots & \vdots & \vdots & \vdots & \vdots & \vdots & \vdots & \vdots & \end{bmatrix}$$

where $C_i = c_i \frac{(1-\upsilon^2)}{Eh}$ $(i = 1, 2, 3, \ldots, N-1)$.

References

Achenbach, J.D., 1973. Wave propagation in elastic solids. North-Holland, Amsterdam.

Chakraborty, A., Sivakumar, M.S., Gopalakrishnan, 2006. Spectral element based model for wave propagation analysis in multi-wall carbon nanotubes. International Journal of Solids and Structures 43, 279–294.

Dong, K., Wang, X., 2006. Wave propagation in carbon nanotubes under large deformation. Nanotechnology 17, 2773–2782.

Eringen, A.C., 1983a. On differential equations of nonlocal elasticity and solutions of screw dislocation and surface waves. Journal of Applied Physics 54, 4703–4710.

Eringen, A.C., 1983b. On differential equations of nonlocal elasticity and solutions of screw dislocation and surface waves. Journal of Applied Physics 54 (9).

Eringen, A.C., Kim, B.S., 1977. Relation between non-local elasticity and lattice dynamics. Crystal Lattice Defects 7, 51.

Fan, S., Chapline, M.G., Franklin, N.R., Tombler, T.W., Cassell, A.M., Dai, H., 1999. Self-oriented regular arrays of carbon nanotubes and their field emission properties. Science 394, 52–55.

Gumbsch, P., 1996. An atomistic study of brittle fracture: toward explicit failure criteria from atomistic modeling. Journal of Materials Research 10, 2897–2907.

Ilcewicz, L., Narasimhan, Wilson, J., 1981. An experimental verification of nonlocal fracture criterion. Engineering Fracture Mechanics 14, 801–808.

Kohlhoff, S., Gumbsch, P., Fischmeister, H.F., 1991. Crack propagation in baa crystals studied with a combined finite element and atomistic model. Philosophical Magazine A 64 (4), 851–878.

Lau, K.T., 2003. Interfacial bonding characteristics of nanotube/polymer composites. Chemical Physics Letters 370, 399–405.

Li, C.Y., Chou, Tsu-Wei, 2003a. A structural mechanics approach for the analysis of carbon nanotubes. International Journal of Solids and Structures 40, 2487–2499.

Li, C.Y., Chou, Tsu-Wei, 2003b. Single-walled carbon nanotubes as ultrahigh frequency nanomechanical resonators. Physics Review B 68, 073405-1–073405-3.

Li, C.Y., Chou, Tsu-Wei, 2004. Vibrational behaviors of multiwalled-carbon-nanotube-based nanomechanical resonators. Applied Physics Letters S 84 (1), 121–123.

Li, C.Y., Chou, Tsu-Wei, 2005. Quantized molecular structural mechanics modeling for studying the specific heat of single-walled carbon nanotubes. Physical Review B 71, 075409-1–075409-6.

Mira Mitra, Gopalakrishnan, S., 2006. Wave propagation analysis in carbon nanotube embedded composite using wavelet based spectral finite element. Smart Materials and Structures 15, 104–122.

Popov, V.N., Doren, V.E.V., 2000. Elastic properties of single-walled carbon nanotube. Physics Review B 61, 3078–3084.

Qian, H., Xu, K.Y., Ru, C.Q., 2005. Curvature effects on axially compressed buckling of a small-diameter double-walled carbon nanotube. International Journal of Solids and Structures 42, 5426–5440.

Reulet, B. et al., 2000. Acoustoelectric effects in carbon nanotubes. Physical Review Letters 85, 2828–2832.

Ru, C.Q., 2000. Column buckling of multiwalled carbon nanotubes with interlayer axial displacements. Physics Review B 62, 16962–16967.

Ru, C.Q., 2001. Axially compressed buckling of a double-walled carbon nanotube embedded in an elastic medium. Journal of the Mechanics and Physics of Solids 49, 1265–1279.

Rueckes, T., Kim, K., Joselevich, E., Tseng, G.Y., Cheung, C.-L., Lieber, C.M., 2000. Carbon nanotube-based nonvolatile random access memory for molecular computing. Science 289, 94–97.

Shen, S., Atluri, S.N., 2004. Multiscale simulation based on meshless local Petrov–Galerkin (MLPG) method. CMES: Computer Modeling in Engineering and Sciences 5 (3), 235–255.

Wang, Q., 2005. Wave propagation in carbon nanotubes via nonlocal continuum mechanics. Journal of Applied Physics 98, 124301.

Wang, Lifeng, Hu, Haiyan, 2005. Flexural wave propagation in single-walled carbon nanotubes. Physical Review B 71, 195412–195419.

Wang, C.Y., Ru, C.Q., Mioduchowski, A., 2003. Axially compressed buckling of pressured multiwall carbon nanotubes. International Journal of Solids and Structures 40, 3893–3911.

Yakobson, B.I., Brabec, C.J., Bernholc, J., 1996. Nanomechanics of carbon tubes instabilities beyond linear range. Physical Review Letters 76, 2511–2514.

Yao, Z., Postma, H.W.C., Balents, L., Dekker, C., 1999. Carbon nanotube intra-molecular junctions. Nature 402, 273–276.

Yoon, J., Ru, C.Q., Mioduchowski, A., 2003. Sound wave propagation in multiwall carbon nanotubes. Journal of Applied Physics 93, 4801–4806.

Yoon, J., Ru, C.O., Mioduchowski, A., 2004. Timoshenko-beam effects on transverse wave propagating in carbon nanotubes. Composites Part B: Engineering 35, 87–93.

Yu, J., Kalia, R.K., Vashishta, P., 1995. Phonons in graphitic tubules: a tight-binding molecular dynamics study. Journal of Chemical Physics 103, 6697–6705.

Zhang, Y.Q., Liu, G.R., Wang, J.S., 2004. Small-scale effects on buckling of multiwalled carbon nanotubes under axial compression. Physical Review B 70, 205430-1–205430-6.

Zhang, Y.Q., Liu, G.R., Han, Xu., 2005a. Transverse vibrations of double-wall carbon nanotubes under compressive axial load. Physics Letters A 340, 258–266.

Zhang, Y.Q., Liu, G.R., Xie, X.Y., 2005b. Free transverse vibrations of double-walled carbon nanotubes using a theory of nonlocal elasticity. Physics Review B 71, 195404-1–195404-7.